Anomalous Subdiffusion Is a Measure for Cytoplasmic Crowding in Living Cells

Matthias Weiss,* Markus Elsner,[†] Fredrik Kartberg,[†] and Tommy Nilsson[†]

*MEMPHYS-Center for Biomembrane Physics, Physics Department, University of Southern Denmark, Campusvej 55, Odense M, Denmark; and [†]Department of Medical Biochemistry, Göteborg University, Medicinaregatan 9A, Göteborg, Sweden

ABSTRACT   Macromolecular crowding dramatically affects cellular processes such as protein folding and assembly, regulation of metabolic pathways, and condensation of DNA. Despite increased attention, we still lack a definition for how crowded a heterogeneous environment is at the molecular scale and how this manifests in basic physical phenomena like diffusion. Here, we show by means of fluorescence correlation spectroscopy and computer simulations that crowding manifests itself through the emergence of anomalous subdiffusion of cytoplasmic macromolecules. In other words, the mean square displacement of a protein will grow less than linear in time and the degree of this anomaly depends on the size and conformation of the traced particle and on the total protein concentration of the solution. We therefore propose that the anomaly of the diffusion can be used as a quantifiable measure for the crowdedness of the cytoplasm at the molecular scale.

INTRODUCTION

At first glance the cytoplasm of mammalian cells appears to be an unstructured, aqueous liquid in which proteins, sugar molecules, and other solvents are dissolved. Taking a closer look, one realizes that the cytoplasm is in fact structured on many length scales: on the μm-scale we find organelles like the mitochondria, endosomes, and the Golgi apparatus. On a smaller scale ($\sim$100 nm) the endoplasmic reticulum (ER) imposes a random reticular network (Marsh et al., 2001) together with the cytoskeletal elements, such as microtubuli and actin filaments. Together, these yield a higher order structure of the cytoplasm (see, for example, Alberts et al., 1994 for a more detailed introduction). As a consequence, diffusional movement of particles, such as macromolecules, can be obstructed. In fact, it has been reported that the diffusional mobility in the cytoplasm strongly decreases with an increasing radius of the tracked particle, leaving particles with a radius >25–30 nm immobile (Luby-Phelps et al., 1986, 1987; Seksek et al., 1997; Arrio-Dupont et al., 2000). Extensive computer simulations also have shown that the molecular mobility is reduced when a particle diffuses in a maze-like environment (Saxton, 1993): When increasing the concentration c of obstacles in the maze, the tracer particles appeared to diffuse slower and slower until complete immobilization occurred beyond a certain value, c^*. Interestingly, when approaching c^* the characteristics of the diffusional motion changed dramatically. The mean square displacement $v(t)$ of the monitored particles did no longer grow linearly in time but, rather, showed a power law $v(t) \sim t^\alpha$

with $\alpha < 1$. This kind of diffusion is known as anomalous subdiffusion and has been found in many different contexts; e.g., for the movement of lipids on model membranes (Schutz et al., 1997), integral membrane proteins on organellar membranes (Weiss et al., 2003) and proteins in the nucleoplasm (Wachsmuth et al., 2000), solute transport in porous media (Drazer and Zanette, 1999), and the translocation of polymers (Metzler and Klafter, 2003; Kantor and Kardar, 2004).

In the case of obstructed diffusion, the emergence of a transitional subdiffusive regime is observed when the concentration of obstacles is increased. This transient subdiffusive behavior collapses back to normal diffusion after a timescale T which diverges in the limit $c \rightarrow c^*$. At $c = c^*$ (the so-called percolation threshold), subdiffusion is observed on all timescales. Whereas T grows with increasing obstacle concentration, the (transient) anomaly parameter α decreases concomitantly from unity to a finite value α^* at c^*, which is given by $\alpha^* \approx 0.697$ and $\alpha^* \approx 0.526$ for two- and three-dimensional environments, respectively (Havlin and Ben-Avraham, 1987; Bouchaud and Georges, 1990). These values were obtained for continuum percolation in a ''Swiss-cheese'' model (see Havlin and Ben-Avraham, 1987 for details) and presumably represent the best approximation to the actual values in nature. However, other mechanisms can also lead to anomalous subdiffusion where the entire range $0 < \alpha < 1$ may be observed (see, for example, Bouchaud and Georges, 1990; Metzler and Klafter, 2000). Regardless of its microscopic origin, anomalous subdiffusion has been shown to strongly influence the formation of spatiotemporal patterns (Weiss, 2003) as well as kinetic rates (Saxton, 2002) and the time course of enzymatic reactions (Berry, 2002).

When neglecting the higher-order structuring of the cytoplasm by cytoskeletal elements and membranes, one could anticipate from the above that one deals with an unstructured aqueous solution in which normal diffusion

should be observed. Yet, the assumption of the cytoplasm as being a homogenous viscous solution is somewhat misleading as differently sized proteins, lipids, and sugars constitute up to 40% of the cytoplasmic volume (Fulton, 1982). This phenomenon is commonly referred to as *molecular crowding* and has recently received increased attention (Ellis and Minton, 2003; Rivas et al., 2004) since, for example, enzymatic reactions and protein folding appear to be strongly affected by the crowdedness (for reviews see Ellis, 2001; Hall and Minton, 2003). Also, crowding seems to contribute significantly to the high viscosity of the cytoplasm which has been determined to be three- to fourfold higher than that of water (Verkman, 2002; Elsner et al., 2003). Despite the increased interest in the phenomena associated with molecular crowding, the term ''crowdedness'' so far has been used without a quantitative definition of what it actually means. In other words, we lack a definition of a quantity which summarizes *how* crowded an environment really is and also states in which primary physical property of the heterogeneous fluid the crowdedness is manifested. As basic criterion, a quantitative measure of crowdedness should be independent of influences imposed by the cytoskeletal and membrane obstacles discussed above. Rather, it should reflect a basic and unambiguous physical quantity which can be assigned to the highly, yet heterogeneous, concentrated protein/sugar solution called cytoplasm.

Here we utilize fluorescence correlation spectroscopy (FCS) to show that inert tracer particles show anomalous subdiffusion in the cytoplasm of living cells over a wide range of particle sizes. This behavior is found to occur irrespective of the stage of the cell cycle or the presence of ER membrane structures and cytoskeletal scaffolds. Using computer simulations, we demonstrate that this effect most likely arises due to molecular crowding, e.g., diffusing particles are scattered by nearby particles due to excluded-volume interactions. We verify our hypothesis in vitro by determining the degree of anomalous diffusion of tracer particles in highly concentrated dextran solutions.

MATERIALS AND METHODS

Cell culture

HeLa cell lines were grown in DMEM supplemented with 10% fetal calf serum, 100 μg/ml penicillin, 100 mg/ml streptomycin, and 10 mM glutamine (Gibco, Eggenstein, Germany). FITC-labeled dextrans of different molecular masses (10, 40, 500, 2000 kDa: Molecular Probes, Eugene, OR; 150 kDa: Sigma, Germany) were either injected with an Eppendorf microinjection system (Eppendorf, Hamburg, Germany) or incorporated by electroporation. Microtubules were disrupted by incubating cells with 20 μM nocodazole at 37°C for one hour. To disrupt the ER network, cells were treated with 5 μg/ml Filipin III (Sigma, Germany) for 30 min at 37°C and 45 min at 30°C. The efficiency of the treatment was confirmed by examining the change of the fluorescence pattern of HeLa cells expressing the ER marker Sec61 fused to CFP (see Axelsson and Warren, 2004 for details). Experiments using mitotic cells were accomplished by arresting HeLa cells in the metaphase of mitosis by incubating them for 16 h

in the presence of 100 nM nocodazole (Sigma Chemical, St. Louis, MO) (Zieve et al., 1980).

For subcellular fractionation, HeLa cells were scraped off the culture dish and collected by centrifugation (500g, 5 min.). Cells were washed with phosphate-buffered saline (PBS) twice and once with homogenization buffer. The homogenization buffer consisted of 20 mM HEPES-KOH (pH 7.4), 1 mM DTT (both Biomol, Hamburg, Germany), 250 mM sucrose (USB, Cleveland, OH), 1 mM EDTA (Merck, Hamburg, Germany), plus protease inhibitors (1 μg/ml aprotinin, 1 μg/ml leupeptin, 1 μg/ml pepstatin, 1 μg/ml antipain, 1 mM Benzamidine-HCl, 40 μg/ml phenylmethylsulfonyl fluoride). Cell pellets were resuspended in 4 volumes of homogenization buffer in the presence of protease inhibitors and homogenized using a ball-bearing homogenizer (10 passages with a 16 μm clearing). The homogenate was then centrifuged sequentially at $10^3 g$ (P1), $10^4 g$ (P10), and at $10^5 g$ (P100), retaining the supernatant at each subsequent centrifugation step. The final $10^5 g$ supernatant (S100) was boiled in equal volume sample buffer and various amounts (0.1–10 μg) of protein were resolved on a 12.5% SDS-polyacrylamide gel. Protein bands were visualized by Coomassie Brilliant blue G250 (Merck, Darmstadt, Germany).

Fluorescence microscopy and FCS

FCS measurements were carried out on a LSM510/ConfoCor 2 (Carl Zeiss, Jena, Germany) using a 488-nm laser line for illumination. The fluorescence was detected with a bandpass filter (505–550 nm) and the objective (Apochromat 40×/1.2 W) was heated to 37°C using an objective heater (Bioptechs, Butler, PA). The pinhole for all shown measurements was 1 Airy unit. We verified that for free diffusion in water, the autocorrelation function of the fluorescence was well fitted by Eq. 1 with $\alpha = 1$. Thus, our analysis does not suffer from deviations of the confocal volume from a three-dimensional Gaussian point-spread function (see also discussions in Hess and Webb, 2002; Weiss et al., 2003). For each cell and condition, at least 30 fluorescence time series of 10 s duration were recorded, autocorrelated, and superimposed for fitting with XMGRACE (see http://plasma-gate.weizmann.ac.il/Grace/).

Autocorrelation times τ_D were translated into apparent hydrodynamic radii by comparison with green fluorescent protein (EGFP, Molecular Probes) in PBS: From the diffusion coefficient $D \approx 85$ μm²/s of GFP in buffer (Terry et al., 1995) and the determined diffusive time $\tau_D = 130$ μs, we obtained via the Einstein-Stokes equation $D = k_B T/(6\pi\eta r)$ a mean radius $r = 2.6$ nm for GFP ($k_B T \approx 4.3 \times 10^{-21}$ J is the thermal energy and $\eta \approx 10^{-3}$ kg/(m × s) is the viscosity of water). This value agrees well with the dimensions derived from the crystal structure of GFP (Yang et al., 1996).

Fitting anomalous diffusion

To determine if the experimentally observed autocorrelation function $C(\tau)$ is governed by anomalous subdiffusion one has to generalize the well-known expression for the autocorrelation decay due to normal diffusion. Knowing the illumination profile (which is usually approximated by a three-dimensional Gaussian), this task is essentially done when the propagator $G(\vec{r}_1, \vec{r}_2, \tau)$ of the density of the (sub)diffusing particles is known. This function simply tells the probability to find a particle at position $\vec{r}_2$ after a time τ when it was initially at position $\vec{r}_1$. For normal diffusion $G(\vec{r}_1, \vec{r}_2, \tau)$ is simply a Gaussian which satisfies the diffusion equation and it is easy to derive the appropriate expression for $C(\tau)$ (for details see, for example, Hess and Webb, 2002; Weiss et al., 2003). In contrast, the propagator for subdiffusion is somewhat more difficult to obtain. Bearing in mind that subdiffusion is commonly defined via the asymptotic power-law increase of the mean square displacement $v(t) \sim t^\alpha$ ($\alpha < 1$), a straight-forward (yet approximative) approach to determine $G(\vec{r}_1, \vec{r}_2, \tau)$ is to assume a time-dependent diffusion coefficient $D(t) = \Gamma t^{\alpha-1}$ so that $v(t) = D(t) \times t$. Clearly, this interpretation is problematic for small times as $D(t)$ diverges for $t \rightarrow 0$. Yet, assuming that one still can use this approximation for all times, one obtains the propagator

$$G(\vec{r}_1, \vec{r}_2, \tau) = \frac{\exp(-|\vec{r}_1 - \vec{r}_2|^2/(\Gamma\tau^{\alpha}))}{\sqrt{\pi\Gamma\tau^{\alpha}}},$$

which satisfies the modified diffusion equation

$$\frac{\partial G(\vec{r}_1, \vec{r}_2, t)}{\partial t} = D(t)\Delta G(\vec{r}_1, \vec{r}_2, t).$$

Using this expression in conjunction with a Gaussian illumination profile, we obtain

$$C(\tau) = \frac{1 + fe^{-\tau/\tau_{\mathrm{T}}}}{(1 + (\tau/\tau_{\mathrm{D}})^{\alpha})\sqrt{1 + (\tau/(S^2\tau_{\mathrm{D}}))^{\alpha}}}. \tag{1}$$

Here, α is the degree of the anomalous subdiffusion, and τ_{D} is the diffusive time which is related to the diffusion coefficient D and the width r_0 of the focus as $\tau_{\mathrm{D}} = r_0^2/(4D)$ for $\alpha = 1$. The parameter S considers the unavoidable extension of the confocal volume along the optical axis, whereas f, τ_{T} are the triplet fraction and time, respectively, which take care of the photophysics on short timescales.

The fitting function Eq. 1 has been used previously to determine anomalous subdiffusion in FCS experiments (Schwille et al., 1999; Wachsmuth et al., 2000; Weiss et al., 2003) and the very same approach served as a starting point to derive fitting functions for quantitative photobleaching experiments (Feder et al., 1996; Saxton, 2001). However, the outlined strategy appears somewhat questionable due to the divergence of the time-dependent diffusion coefficient on short timescales. A mathematically correct treatment of the problem therefore has to employ a fractional Fokker-Planck equation (FFPE), i.e., a sophisticated extension of the normal diffusion equation. For the FFPE one can analytically calculate the propagator in terms of Fox functions for all $\alpha < 1$ (see Metzler and Klafter, 2000). From this, one could derive $C(\tau)$ analytically. However, the emerging function only has a limited value for a later fitting procedure as its complexity severely hampers the fitting to experimental data. We therefore have chosen a different approach: Using the series expansions of the propagator (cf. Metzler and Klafter, 2000), we calculated numerically the propagator and the resulting correlation function. We then fitted these curves with Eq. 1 (fixing the triplet fraction to $f = 0$) to test if the obtained value α_{fit} corresponds to the value α_{FPE} imposed in the FFPE. In all cases, Eq. 1 yielded a good fit to the $C(\tau)$ as obtained from the FFPE (see Fig. 1 for a representative example). The anomaly degrees α_{fit} and α_{FPE} on the other hand were slightly different (Fig. 1, *inset*) and a linear regression yielded $\alpha_{\mathrm{fit}} = 1.1 \times \alpha_{\mathrm{FPE}} - 0.12$. In the range $0.5 \leq \alpha \leq 1$ the deviations between Eq. 1 and the FFPE is therefore <10% which is within the accuracy of the experimental data. In view of this and due to its much simpler use in the fitting procedure, we have chosen to always use Eq. 1 for fitting.

Computer simulations

To investigate the effect of crowdedness by means of computer simulations, we considered a cubic probe volume with linear extension L and periodic boundary conditions. In total, $N = 5000$ spherical particles/proteins having molecular masses in the range 50 kD–1 MDa were positioned at random locations in the probe volume. By changing L we were able to change the apparent concentration of particles. To consider excluded volume effects, we imposed a soft-core potential between the particles, which is common for mesoscopic simulations (Nikunen et al., 2003): Each particle k experienced a (repulsive) force $\vec{f}_{ik} = A(1 - d/r_{\mathrm{c}})\vec{e}_{ik}$ from a neighboring molecule i along the vector $\vec{e}_{ik}$ pointing from particle k to particle i. Here, d measures the distance between the particles i, k, minus the radii r_i, r_k of the two particles. For $d > r_{\mathrm{c}}$ the particles do not meet and thus $\vec{f}_{ik} = \vec{f}_{ki} = 0$. Besides this excluded volume interaction, all particles were also subject to thermal noise,
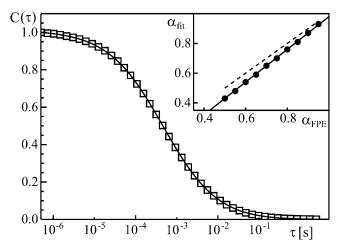

FIGURE 1 The autocorrelation curve $C(\tau)$ obtained for subdiffusive motion in the framework of a FFPE ($\alpha_{\mathrm{FPE}} = 0.65$, *open symbols*) is well described by a fit with Eq. 1 ($\alpha_{\mathrm{fit}} = 0.59$, *full line*). (*Inset*) The actual value α_{fit} for the anomaly obtained by this fitting (*closed symbols*) slightly deviates from the value α_{FPE} imposed in the FFPE (*dashed line*). The dependence is best described by $\alpha_{\mathrm{fit}} = 1.1\alpha_{\mathrm{FPE}} - 0.12$ (*full line*).

i.e., for each time step Δt the new position emerged from the old one via the (overdamped) Langevin equation $\vec{x}_i(t + \Delta t) = \vec{\xi} + \Delta t\sum_k \vec{f}_{ik}/\gamma_i$. Here, ξ is Gaussian random number with variance $2D_i\Delta t$ and the friction of the particle is assumed to be given by Stoke's formula ($\gamma_i = 6\pi\eta r_i$) from which one also obtains the diffusion coefficient via $D_i = k_{\mathrm{B}}T/\gamma_i$. The radii were calculated from the imposed molecular mass m_i via the empiric formula $r_i = (8m_i/50)^{1/3}$ nm. This relation has been derived by considering that BSA ($m = 66$ kDa) is approximately globular and has an apparent radius of 2 nm. The distribution $p(m)$ of molecular weights m was taken to be either a Poissonian or uniform (see main text), and a upper cutoff at $m = 1$ MDa was imposed. Before monitoring the diffusional motion, the particles were allowed to equilibrate for 5000 time steps. The remaining parameters were $\Delta t = 10^{-9}$ s, $r_{\mathrm{c}} = 2$ nm, $A/(6\pi\eta) = 10^3$ μm^2/s.

RESULTS

We first monitored with FCS the diffusional motion of fluorescently labeled dextrans in PBS to verify that we observe normal diffusion under these conditions. Indeed, fitting the experimental data with Eq. 1 yielded $\alpha = 1 \pm 0.05$ which indicates that finding anomalous subdiffusion with our setup is not an artifact of a distorted confocal volume (Hess and Webb, 2002; see also discussion in Weiss et al., 2003). Representative autocorrelation curves $C(\tau)$ for dextrans of different molecular weight are shown in Fig. 2. The measurements in PBS also allowed us to determine the apparent hydrodynamic radius r_{H} of the particles (see Methods). In the inset of Fig. 2 we show the increase of the radii for increasing molecular weight m ($r_{\mathrm{H}} \sim m^{0.4}$). In fact, the radii increase slower than anticipated for a simple random-coil polymer for which a description as a linear Gaussian chain yields $r_{\mathrm{H}} \sim m^{0.5}$ (Doi, 1996). This deviation is in agreement with previous reports (Cheng et al., 2002) and may be explained by the fact that dextrans become strongly branched polymers when their mass increases (Nordmeier, 1993).
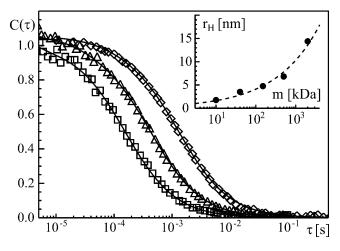
FIGURE 2 Representative autocorrelation curves for dextran in PBS (*squares, triangles, diamonds*: molecular masses $m = 10$ kDa, 150 kDa, 2 MDa, respectively). Best fits according to Eq. 1 (*full lines*) always resulted in $\alpha \approx 1$, indicating normal diffusion. (*Inset*) The hydrodynamic radius r_H as extracted from the diffusive time τ_D of the autocorrelation decay increases approximately as $r_H \sim m^{0.4}$ (*dashed line*).

We next investigated the motion of labeled dextrans in the cytoplasm of HeLa cells in interphase. Representative examples for the obtained autocorrelation curves $C(\tau)$ are shown in Fig. 3. In strong contrast to the behavior in PBS, all dextrans showed subdiffusive motion in cytoplasm albeit with varying degrees of the anomality parameter α. Moreover, the characteristic timescales τ_D of the autocorrelation decays were increased with respect to the ones found for PBS which indicates an overall decrease of the diffusional mobility. Surprisingly, the determined degrees of anomaly α did not correlate linearly with the hydrodynamic sizes of the
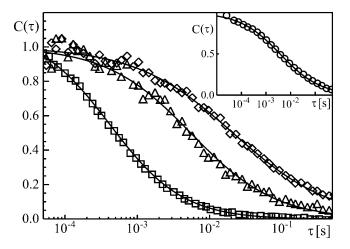

FIGURE 3 Representative autocorrelation curves for dextran in the cytoplasm of living cells in interphase (*squares, triangles, diamonds*: molecular masses 10 kDa, 150 kDa, 2 MDa, respectively). Best fits according to Eq. 1 (*full lines*) revealed that all dextrans moved subdiffusively ($\alpha = 0.86, 0.74, 0.64$; *from left*). (*Inset*) A FITC-labeled IgG antibody ($m = 150$ kDa, $r_H \approx 5.5$ nm) also showed strong subdiffusion ($\alpha \approx 0.55$).

dextran particles (see Table 1). Rather, we observed a very strong subdiffusive motion for small dextrans (40 kDa) which relaxed for increasing mass (500 kDa) and then became stronger again (2 MDa). We next verified that the observed subdiffusion in cytoplasm was not a particular feature of dextran by monitoring the diffusion of a FITC-labeled IgG antibody ($m \approx 150$ kDa) in cytoplasm. Having an apparent hydrodynamic radius $r_H \approx 5.5$ nm (cf. also Arrio-Dupont et al., 2000), we expected IgG to show a similar degree of subdiffusion as seen with 150 kDa dextran ($r_H \approx 5$ nm). In fact, we observed a stronger anomaly ($\alpha \approx 0.55$, see also Fig. 3, *inset*), which may be explained by the fact that an IgG has a different shape than a 150 kDa dextran in solution.

We hypothesized that molecular crowding may have caused the observed anomalous subdiffusion rather than obstruction by cytoskeletal elements or membrane structures. To test for the validity of this assumption, we monitored the diffusional properties of a selection of dextrans in i), nocodazole-treated; ii), latrunculin-treated; iii), Filipin-treated; and iv), mitotic cells. In cases i and ii the microtubules and actin filaments are depolymerized, respectively, whereas in case iii the ER membrane is broken down and other membrane structures like the Golgi apparatus are not affected (Axelsson and Warren, 2004). In case iv the interior of the cell has undergone major changes due to the impending cell division, e.g., the microtubules form a spindle rather than an astral array. In agreement with our hypothesis, the subdiffusion persisted in all cases with similar values for α (see summary in Table 2). This provides strong evidence that obstruction by higher-order structures is not the major cause of the observed subdiffusion. Rather, the observed subdiffusion is caused by molecular crowding.

To obtain further evidence for if and when molecular crowding can cause the emergence of subdiffusion, we used computer simulations of spherical soft-core molecules subject to thermal noise and excluded volume effects (see Methods). To be able to model the cytoplasmic environment, we had to first get an idea about the distribution of protein masses/sizes in the cytoplasm of mammalian cells. We therefore analyzed purified HeLa cytosol by SDS page and Coomassie staining (see Methods). The resulting distribution of molecular weights $p(m)$ is shown in Fig. 4 *a* and is most consistent with a Poisson distribution with a mean $\langle m \rangle = 80$ kDa. Bearing in mind that the used approach actually overestimates the fraction of small proteins due to the denaturing conditions in the gel (protein

TABLE 1 Summary of masses m, hydrodynamic radii r_H (in PBS), and anomalies α and diffusive times τ_D of dextrans in the cytoplasm of living cells

m	r_H	α	τ_D
10 kDa	1.8 nm	0.84 ± 0.04	0.39 ± 0.05 ms
40 kDa	3.5 nm	0.59 ± 0.04	2.9 ± 1.3 ms
150 kDa	4.8 nm	0.73 ± 0.03	6.1 ± 1.9 ms
500 kDa	6.8 nm	0.82 ± 0.05	3.1 ± 1 ms
2 MDa	14.4 nm	0.71 ± 0.04	15.9 ± 4.5 ms

TABLE 2 Summary of the found degrees of anomaly α and diffusive times τ_D in the cytoplasm of living cells under various treatments

m	Interphase α, τ_D	Mitotic α, τ_D	Filipin α, τ_D	Nocodazole α, τ_D	Latrunculin α, τ_D
10 kDa	0.87 ± 0.03	0.74 ± 0.02	0.74 ± 0.06	0.76 ± 0.07	0.74 ± 0.05
	0.39 ± 0.05 ms	0.39 ± 0.06 ms	0.55 ± 0.26 ms	0.34 ± 0.03 ms	1.8 ± 0.06 ms
150 kDa	0.73 ± 0.03	0.75 ± 0.04	0.83 ± 0.04	0.76 ± 0.06	0.76 ± 0.05
	6.1 ± 1.9 ms	1.7 ± 0.6 ms	2.2 ± 0.8 ms	7.8 ± 4.3 ms	1.9 ± 0.3 ms
500 kDa	0.82 ± 0.05	0.75 ± 0.06	0.76 ± 0.05	0.79 ± 0.04	0.76 ± 0.03
	3.1 ± 0.9 ms	5.6 ± 1.3 ms	3.2 ± 0.7 ms	2.7 ± 0.5 ms	3.3 ± 0.2 ms

complexes are disrupted), we tested two distributions in the simulations which were inspired by the experimental distribution $p(m)$ (see Fig. 4 a): i), a Poisson distribution with $\langle m \rangle = 350$ kDa, and ii), a uniform distribution. In both cases we only considered proteins with masses up to 1 MDa and, for simplicity, assumed the proteins to be globular. In both simulation settings, we observed a size-dependent emergence of anomalous subdiffusion which also clearly depended on the fractional volume occupied by the globular proteins (''excluded volume''). In Fig. 4 b we show
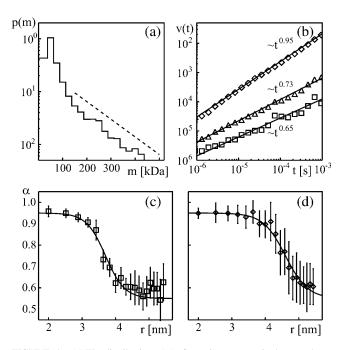

FIGURE 4 (a) The distribution $p(m)$ of protein masses m in the cytoplasm of HeLa cells (see Methods) is well described by a Poissonian (*dashed line*, mean $\langle m \rangle = 80$ kDa). Due to the denaturing conditions of the gel, the fraction of low protein masses is overestimated and can be expected to be significantly higher in reality. (b) Average mean square displacement $v(t)$ for globular proteins with radii 2 nm, 3.6 nm, and 5.4 nm (from top) as obtained by simulations using a Poissonian weight distribution (mean $\langle m \rangle = 350$ kDa to soften the overestimation of low masses). The proteins occupied a fractional volume of 13%. Dashed lines highlight the power-law increase $v(t) \sim t^{\alpha}$. (c) Using the same parameters, the anomaly parameter α is seen to decrease for increasing particle radii r. The full line is a guide to the eye. (d) Same as in (c) for a uniform distribution of molecular weights (50 kDa $\leq$ $m \leq$ 1MDa). Here, a similar decrease of α is observed, yet it occurs for higher values of r and a lower fractional volume occupied by the proteins (7%).

representative curves for the mean square displacement obtained for scenario i, i.e., a Poissonian distribution of molecular masses, at an excluded volume of 13%. Although small proteins were still diffusing more or less normally, the big particles clearly moved subdiffusively. This size-dependence is further highlighted in Fig. 4 c, where one can observe the decrease of the anomaly parameter α with increasing effective particle size. This result was only slightly altered in scenario ii, i.e., for a uniform size distribution. The decrease of α with increasing radii persisted (Fig. 4 d) albeit occurring at bigger radii and at lower values for the excluded volume (7% instead of 13%). As both settings yielded the same gross features, we conclude that an excluded volume interaction (= molecular crowding) likely explains the subdiffusion observed in the cytoplasm of living cells. The successful simulations of course only represent the simplest possible configuration due to the use of globular particles. To quantitatively explain the experimentally observed α-values, a more detailed approach may be necessary which includes, for example, the polymeric nature of the probe (see also Discussion).

To verify the simulation results and consistently test if the mere effect of crowding can cause anomalous subdiffusion, we also studied the diffusional properties of some labeled dextrans (10 kDa, 40 kDa, 500 kDa) in aqueous solution when varying the molar percentages of macromolecules (unlabeled dextran in the range 60–90 kDa; from Acros Organics, Geel, Belgium) to hinder diffusion. As these artificially created crowded fluids were intended to mimic the cytoplasm of living cells, we expected to observe an overall correlation of the α-values between in vitro and in vivo experiments using a particular probe. Consistent with our findings in vivo (the cytoplasm), we observed an increase of the diffusional time τ_D and a concomitant decrease of the anomaly parameter α for the tested dextrans when the concentration C of unlabeled dextran (i.e., the crowding) in the solution was increased (Fig. 5). These experiments also confirmed the simulation results, i.e., the interaction via excluded volume can cause subdiffusion. In accordance with the results in living cells, we again observed that 40 kDa dextran appeared to be much more subdiffusive than its 500 kDa counterpart. We speculate that in both cases this may be caused by a partial reptational movement of the fairly short 40 kDa polymer whereas the more heavy dextrans may be more globular and are thus less prone to reptation (see also Discussion). Nevertheless, we
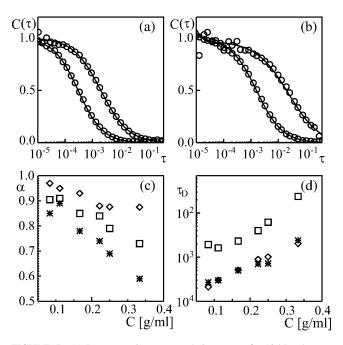
FIGURE 5   (*a*) Representative autocorrelation curves for 10 kDa dextran in solutions with different crowdedness due to dissolved unlabeled dextran (0.08 and 0.25 g/ml, from left). A shift and stretching of $C(\tau)$ is visible for increasing crowdedness. (*b*) Same as in *a* but for 500 kDa dextran. (*c*) The anomality parameter α decreases with increasing crowdedness as measured by the macromolecular concentration (*diamonds*, 10 kDa; *asterisks*, 40 kDa; *squares*, 500 kDa). (*d*) The diffusive time τ_D concomitantly increases with increasing macromolecular concentration, indicating an increase of the effective viscosity. For better visibility error bars have been omitted.

conclude that the degree of anomalous diffusion (α) is a direct reflection of molecular crowding. By comparing in vivo measurements with those in vitro, one can therefore use the determined α-values as a measure for molecular crowding.

DISCUSSION

In summary, we have determined with FCS that inert tracer particles show anomalous subdiffusion in the cytoplasm of mammalian cells. As the occurrence of subdiffusion was not altered in cells where cytoskeletal or organellar membrane architecture have been disrupted, we conclude that the observed subdiffusion is due to molecular crowding. In support of this view, we showed with simulations that subdiffusion naturally arises in a concentration-dependent manner in a system where particles are subject to Brownian motion and only interact via excluded volumes. We further verified these simulation results by monitoring the emergence of subdiffusion in highly concentrated dextran solutions. Thus, we have provided strong evidence that molecular crowding causes anomalous subdiffusion in the cytoplasm of living cells.

It is likely that the observed subdiffusion only persists for intermediate times and that normal diffusion is reencountered for asymptotically large times. For example, in our

simulations we observed via the growth of the mean square displacement $v(t)$ that even for a fairly low excluded volume subdiffusion transiently emerged on scales $t < 1$ μs and then collapsed back to normal diffusion. For increasing particle concentration this subdiffusive regime eventually extended beyond the 1 ms-scale (cf. Fig. 4). Similar phenomena are, for example, also found for obstructed diffusion with immobile obstacles near to the percolation threshold (Saxton, 2001) or for reptating polymers (Doi, 1996). Bearing this in mind, our results do not contradict but rather complement previous studies on cytoplasmic diffusion by means of photobleaching techniques (Seksek et al., 1997; Arrio-Dupont et al., 2000) which employ larger spatial and temporal scales than in FCS and therefore potentially miss the regime of subdiffusion.

In regards to the nature of the used probe, we observed that small dextran molecules can exhibit a much stronger anomalous subdiffusion than their more heavy counterparts (cf. Table 1 and Fig. 5). The most likely explanation for this phenomenon is a (partially) reptational movement of small dextrans. In the ideal case, reptation yields $\alpha = 0.5$ (Doi, 1996) whereas obstructed diffusion of globular particles typically yields a higher value for α (see Introduction). For our case, we propose that small dextrans adopt a ''snake-like'' conformation whereas the more heavy dextrans are more globular and thus are rather subject to obstructed diffusion than reptation. This reasoning is supported by the fact that fructan, a close relative to dextran, was shown to behave like a random-coil polymer for masses $m \ll 100$kDa, whereas above 100 kDa it appeared more like a globule (Kitamura et al., 1994). This reasoning appears even more plausible when bearing in mind that the conformation of (bio)polymers can depend critically on the solvent and that dextrans show strong branching when their mass increases (Nordmeier, 1993). Of course, for reptational movement the simple picture used in the simulations becomes invalid and has to be replaced by a more elaborate polymer model in a heterogeneous environment. It will be interesting to study the crossover from reptation to obstructed diffusion in more detail (M. Weiss et al., unpublished results).

Despite the caveat that the observed subdiffusion may be a transient feature, it is still likely to play a major role in cytoplasmic processes. In our approach with FCS, we observed subdiffusion on a scale of ~500 nm (the diameter of the confocal volume), a scale which is ~100-fold bigger than the typical radius of a globular protein and almost corresponds to the typical size of an *Escherichia coli* bacterium. At least on this scale, anomalous diffusion can greatly modulate the interaction of proteins, e.g., in reaction networks (Berry, 2002; Saxton, 2002) and maybe in protein folding (Ellis, 2001; Hall and Minton, 2003).

Most importantly, the described emergence of subdiffusion provides a means to define a quantitative measure to what crowdedness actually means. In fact, the term ''crowdedness'' by its mere literal sense signals that the

size and conformation of a test particle dictates if it feels an environment as being crowded. Being a water molecule, the cytoplasm does not appear to be any more crowded than any other solution. However, for a macromolecule, and even more for a polymer-like dextran, the cytoplasm with all its embedded proteins provides an obstacle-rich environment. We therefore propose that the degree of anomaly α can serve as a size- and conformation-dependent quantity to characterize the concentration/composition of a heterogeneous solution like the cytoplasm. In other words, by using a defined and standardized set of in vitro solutions (where the composition is varied), it should be feasible to use the degree of anomaly α as a quantitative measure to probe molecular crowding in vivo, be it in the cytoplasm, the nucleus, or other cellular or extracellular environments.

REFERENCES

Alberts, B., D. Bray, J. Lewis, M. Raff, K. Roberts, and J. D. Watson. 1994. Molecular Biology of the Cell, 3rd ed. Garland Publishing, New York.

Arrio-Dupont, M., G. Foucault, M. Vacher, P. F. Devaux, and S. Cribier. 2000. Translational diffusion of globular proteins in the cytoplasm of cultured muscle cells. *Biophys. J.* 78:901–907.

Axelsson, M. A., and G. Warren. 2004. Rapid, ER-independent diffusion of the mitotic Golgi haze. *Mol. Biol. Cell.* 15:1843–1852.

Berry, H. 2002. Monte Carlo simulations of enzyme reactions in two dimensions: fractal kinetics and spatial segregation. *Biophys. J.* 83:1891–1901.

Bouchaud, J. P., and A. Georges. 1990. Anomalous diffusion in disordered media—statistical mechanisms, models, and physical applications. *Physics Rep.* 195:127–293.

Cheng, Y., R. K. Prud'homme, and J. L. Thomas. 2002. Diffusion of mesoscopic probes in aqueous polymer solutions measured by fluorescence recovery after photobleaching. *Macromolecules.* 35:8111–8121.

Doi, M. 1996. Introduction to Polymer Physics. Clarendon Press, Oxford.

Drazer, G., and D. H. Zanette. 1999. Experimental evidence of power-law trapping-time distributions in porous media. *Phys. Rev. E.* 60:5858–5864.

Ellis, R. J. 2001. Macromolecular crowding: obvious but underappreciated. *Trends Biochem. Sci.* 26:597–604.

Ellis, R. J., and A. P. Minton. 2003. Cell biology: join the crowd. *Nature.* 425:27–28.

Elsner, M., H. Hashimoto, J. C. Simpson, D. Cassel, T. Nilsson, and M. Weiss. 2003. Spatiotemporal dynamics of the copi vesicle machinery. *EMBO Rep.* 4:1000–1004.

Feder, T. J., I. Brust-Mascher, J. P. Slattery, B. Baird, and W. W. Webb. 1996. Constrained diffusion or immobile fraction on cell surfaces: a new interpretation. *Biophys. J.* 70:2767–2773.

Fulton, A. B. 1982. How crowded is the cytoplasm? *Cell.* 30:345–347.

Hall, D., and A. P. Minton. 2003. Macromolecular crowding: qualitative and semiquantitative successes, quantitative challenges. *Biochim. Biophys. Acta.* 1649:127–139.

Havlin, S., and D. Ben-Avraham. 1987. Diffusion in disordered media. *Adv. Phys.* 36:695–798.

Hess, S. T., and W. W. Webb. 2002. Focal volume optics and experimental artifacts in confocal fluorescence correlation spectroscopy. *Biophys. J.* 83:2300–2317.

Kantor, Y., and M. Kardar. 2004. Anomalous dynamics of forced translocation. *Phys. Rev. E.* 69:021806.

Kitamura, S., T. Hirano, K. Takeo, M. Mimura, K. Kajiwara, T. Stokke, and T. Harada. 1994. Conformation of $(2 \rightarrow 1)$-β-d-fructan in aqueous solution. *Int. J. Biol. Macromol.* 16:313–317.

Luby-Phelps, K., P. E. Castle, D. L. Taylor, and F. Lanni. 1987. Hindered diffusion of inert tracer particles in the cytoplasm of mouse 3t3 cells. *Proc. Natl. Acad. Sci. USA.* 84:4910–4913.

Luby-Phelps, K., D. L. Taylor, and F. Lanni. 1986. Probing the structure of cytoplasm. *J. Cell Biol.* 102:2015–2022.

Marsh, B. J., D. N. Mastronarde, K. F. Buttle, K. E. Howell, and J. R. McIntosh. 2001. Organellar relationships in the Golgi region of the pancreatic beta cell line, hit-t15, visualized by high resolution electron tomography. *Proc. Natl. Acad. Sci. USA.* 98:2399–2406.

Metzler, R., and J. Klafter. 2000. The random walk's guide to anomalous diffusion: a fractional dynamics approach. *Physics Rep.* 339:1–77.

Metzler, R., and J. Klafter. 2003. When translocation dynamics becomes anomalous. *Biophys. J.* 85:2776–2779.

Nikunen, P., M. Karttunen, and I. Vattulainen. 2003. How would you integrate the equations of motion in dissipative particle dynamics simulations? *Comp. Phys. Comm.* 153:407–423.

Nordmeier, E. 1993. Static and dynamic light-scattering solution behavior of pullulan and dextran in comparison. *J. Phys. Chem.* 97:5770–5785.

Rivas, G., F. Ferrone, and J. Herzfeld. 2004. Life in a crowded world. *EMBO Rep.* 5:23–27.

Saxton, M. J. 1993. Lateral diffusion in an archipelago. Dependence on tracer size. *Biophys. J.* 64:1053–1062.

Saxton, M. J. 2001. Anomalous subdiffusion in fluorescence photobleaching recovery: a Monte Carlo study. *Biophys. J.* 81:2226–2240.

Saxton, M. J. 2002. Chemically limited reactions on a percolation cluster. *J. Chem. Phys.* 116:203–208.

Schutz, G. J., H. Schindler, and T. Schmidt. 1997. Single-molecule microscopy on model membranes reveals anomalous diffusion. *Biophys. J.* 73:1073–1080.

Schwille, P., J. Korlach, and W. W. Webb. 1999. Fluorescence correlation spectroscopy with single-molecule sensitivity on cell and model membranes. *Cytometry.* 36:176–182.

Seksek, O., J. Biwersi, and A. S. Verkman. 1997. Translational diffusion of macromolecule-sized solutes in cytoplasm and nucleus. *J. Cell Biol.* 138:131–142.

Terry, B. R., E. K. Matthews, and J. Haseloff. 1995. Molecular characterization of recombinant green fluorescent protein by fluorescence correlation microscopy. *Biochem. Biophys. Res. Commun.* 217:21–27.

Verkman, A. S. 2002. Solute and macromolecule diffusion in cellular aqueous compartments. *Trends Biochem. Sci.* 27:27–33.

Wachsmuth, M., W. Waldeck, and J. Langowski. 2000. Anomalous diffusion of fluorescent probes inside living cell nuclei investigated by spatially-resolved fluorescence correlation spectroscopy. *J. Mol. Biol.* 298:677–689.

Weiss, M. 2003. Stabilizing turing patterns with subdiffusion in systems with low particle numbers. *Phys. Rev. E.* 68:036213.

Weiss, M., H. Hashimoto, and T. Nilsson. 2003. Anomalous protein diffusion in living cells as seen by fluorescence correlation spectroscopy. *Biophys. J.* 84:4043–4052.

Yang, F., L. G. Moss, and G. N. Phillips. 1996. The molecular structure of green fluorescent protein. *Nat. Biotechnol.* 14:1246–1251.

Zieve, G. W., D. Turnbull, J. M. Mullins, and J. R. McIntosh. 1980. Production of large numbers of mitotic mammalian cells by use of the reversible microtubule inhibitor nocodazole. Nocodazole accumulated mitotic cells. *Exp. Cell Res.* 126:397–405.